
SecureFedYJ: a safe feature Gaussianization protocol for Federated Learning

Tanguy Marchand
Owkin Inc., New York, USA.
tanguy.marchand@owkin.com

Boris Muzellec
Owkin Inc., New York, USA.
boris.muzellec@owkin.com

Constance Beguier*
constancebeguier@gmail.com

Jean Ogier du Terrail
Owkin Inc., New York, USA.
jean.du-terrail@owkin.com

Mathieu Andreux
Owkin Inc., New York, USA.
mathieu.andreux.com

Abstract

The Yeo-Johnson (YJ) transformation is a standard parametrized per-feature unidimensional transformation often used to Gaussianize features in machine learning. In this paper, we investigate the problem of applying the YJ transformation in a cross-silo Federated Learning setting under privacy constraints. For the first time, we prove that the YJ negative log-likelihood is in fact convex, which allows us to optimize it with exponential search. We numerically show that the resulting algorithm is more stable than the state-of-the-art approach based on the Brent minimization method. Building on this simple algorithm and Secure Multiparty Computation routines, we propose SECUREFEDYJ, a federated algorithm that performs a pooled-equivalent YJ transformation without leaking more information than the final fitted parameters do. Quantitative experiments on real data demonstrate that, in addition to being secure, our approach reliably normalizes features across silos as well as if data were pooled, making it a viable approach for safe federated feature Gaussianization.

1 Introduction

Federated Learning (FL) [45, 32] is an approach that was recently proposed to train machine learning (ML) models across multiple data holders, or *clients*, without centralizing data points, notably for privacy reasons. While many FL applications have been proposed, two main settings have emerged [23]: cross-device FL, involving a large number of small edge devices, and cross-silo FL, dealing with a smaller number of clients, with larger computational capabilities. Due to the sensitivity and relative local scarcity of medical data, healthcare is a promising application of cross-silo FL [40], e.g. to train a biomedical ML model between different hospitals as if all the datasets were pooled in a central server. In this paper, we focus on the cross-silo setting.

The constraints of cross-silo FL Although cross-silo FL resembles standard distributed learning, it faces at least two important distinct challenges: privacy and heterogeneity. Due to data sensitivity, clients might impose stringent security and privacy constraints on FL collaborations. This arises in

*Contribution done while at Owkin, Inc.

cooperative FL projects, where models are jointly trained on industrial competitors’ datasets [55], as well as medical FL applications, where conservative data regulations might apply. In this setting, using standard FL algorithms such as FEDAVG [32] might not provide enough privacy guarantees, as privacy attacks such as data reconstruction can be carried out based on the clients’ gradients [56, 54]. Various protocols based on Secure Multiparty Computation (SMC) (see Section 2 for more details), such as Secure Aggregation [4], can mitigate this shortcoming by disclosing only the sum of the gradients from all clients to the server, without disclosing each gradient individually.

An additional constraint is that data might present statistical heterogeneity across clients, i.e. the local clients’ data distributions may not be identical. In the case of medical applications, such heterogeneity may be caused e.g. by environmental variations or differences in the material that was used for acquisition [43, 47, 2]. While different ways of adapting federated training algorithms have been proposed to automatically tackle heterogeneity [28, 29, 24], these solutions do not address data harmonization and normalization prior to FL training.

Preprocessing in ML Data preprocessing is a crucial step in many ML applications, leading to important performance gains. Among others, common preprocessing methods include data whitening, principal component analysis (PCA) [22] or zero component analysis [27, 20, 46]. However, linear normalization methods might not suffice when the original data distribution is highly non-Gaussian. For tabular and time series data, a popular approach to Gaussianize the marginal distributions is to apply feature-wise non-linear transformations. Two commonly-used parametric methods are the Box-Cox [5] transformation and its extension, the Yeo-Johnson (YJ) transformation [52]. Both have been used in multiple applications, such as climate and weather forecast [53, 50, 51], economics [13] and genomic studies [7, 58, 9].

Problem and contributions In this paper, we investigate the problem of data normalization in the cross-silo FL setting, by exploring how to apply the YJ transformation to a distributed dataset. This problem arises frequently in medical cross-silo FL, e.g. when trying to jointly train models on genetic data (see e.g. [19, 57]). Due to data heterogeneity, no single client can act as a reference client: indeed, there is no guarantee that transformation parameters fitted on a single client would be relevant for other clients’ data. Hence, it is necessary to fit normalization methods on the full federated dataset. Moreover, in this setting, data privacy is of paramount importance, and therefore FL protocols should be carefully designed. Our main contributions to this problem are as follows:

1. We prove that the negative YJ log-likelihood is convex (Section 3), which is a novel result, to the best of our knowledge.
2. Building on this property, we introduce EXPYJ, a method to fit the YJ transformation based on exponential search (Section 3). We numerically show that this method is more stable than standard approaches for fitting the YJ transformation based on the Brent minimization method [6].
3. We propose SECUREFEDYJ (Section 4), a secure way to extend EXPYJ in the cross-silo FL setting using SMC. We show that SECUREFEDYJ does not leak any information on the datasets apart from what is leaked by the parameters minimizing the YJ negative log-likelihood (Section 4 and Proposition 4.1). By construction, SECUREFEDYJ provides the same results as the pooled-equivalent EXPYJ, regardless of how the data is split across the clients. We check this property in numerical experiments (Section 4). The core ideas behind the resulting algorithm, SECUREFEDYJ, are summarised in Figure 7.

Finally, we illustrate our contributions in numerical applications on synthetic and genomic data in Section 5.

2 Background

The Yeo-Johnson transformation The YJ transformation [52] was introduced in order to Gaussianize data that can be either positive or negative. It was proposed as a generalization of the Box-Cox transformation [5], that only applies to non-negative data. The YJ transformation consists in applying to each feature a monotonic function $\Psi(\lambda, \cdot)$ parametrized by a scalar λ , independently of the other features. Thus, there are as many λ ’s as there are features. For a real number x , $\Psi(\lambda, x)$ is defined as:

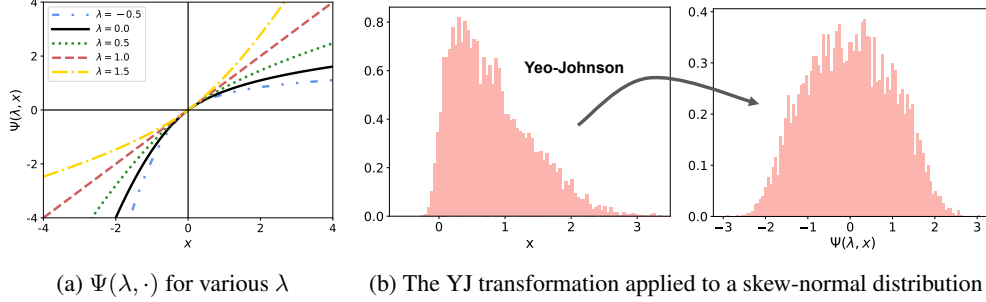


Figure 1: The Yeo-Johnson transformation applies a 1-D univariate transform to Gaussianize data.

$$\Psi(\lambda, x) = \begin{cases} [(x+1)^\lambda - 1]/\lambda, & \text{if } x \geq 0, \lambda \neq 0, \\ \ln(x+1), & \text{if } x \geq 0, \lambda = 0, \\ -[(-x+1)^{2-\lambda} - 1]/(2-\lambda), & \text{if } x < 0, \lambda \neq 2, \\ -\ln(-x+1), & \text{if } x < 0, \lambda = 2. \end{cases} \quad (1)$$

Figure 1a shows the shape of the YJ function for various values of λ .

The Yeo-Johnson likelihood Let us consider real-valued samples $\{x_i\}_{i=1, \dots, n}$, and let us apply the YJ transformation $\Psi(\lambda, \cdot)$ to these samples to Gaussianize their distribution. The log-likelihood that $\{\Psi(\lambda, x_i)\}_{i=1, \dots, n}$ comes from a Gaussian with mean μ and variance σ^2 is given by (derivation details are provided in Appendix A.1):

$$\log \mathcal{L}_{\text{YJ}}(\lambda, \sigma^2, \mu) = -\frac{n}{2} \log(2\pi\sigma^2) - \frac{1}{2\sigma^2} \sum_{i=1}^n [\Psi(\lambda, x_i) - \mu]^2 + (\lambda - 1) \sum_{i=1}^n \text{sgn}(x_i) \log(|x_i| + 1).$$

For a given λ , the log-likelihood is maximized for $\mu_* = \frac{1}{n} \sum_{i=1}^n \Psi(\lambda, x_i)$ and $\sigma_*^2 = \frac{1}{n} \sum_{i=1}^n (\Psi(x_i, \lambda) - \mu_*)^2$. Once we replace μ and σ^2 by μ_* and σ_*^2 , it becomes:

$$\log \mathcal{L}_{\text{YJ}}(\lambda) = -\frac{n}{2} \log(\sigma_{\Psi(\lambda, \{x_i\})}^2) + (\lambda - 1) \sum_{i=1}^n \text{sgn}(x_i) \log(|x_i| + 1) - \frac{n}{2} \log(2\pi), \quad (2)$$

see [52]. Maximizing the YJ log-likelihood is therefore a 1-dimensional problem for each feature. Once the optimal λ_* is found, the transformed data $\Psi(\lambda, x_i)$ is usually renormalized by subtracting its empirical mean μ_* and dividing by the square root of its empirical variance σ_*^2 . Figure 1b shows an example of the YJ transformation applied to a skew-normal distribution. Note that in a typical application, the triplet $(\lambda_*, \mu_*, \sigma_*^2)$ is fitted on the training data only, and is then used to Gaussianize the test dataset during inference.

Minimization methods in dimension 1 As seen above, fitting a YJ transformation can be reduced to a 1D optimization problem. To tackle this problem, we introduce two standard 1D minimization methods: (i) Brent minimization [6] and (ii) exponential search [3].

Brent minimization [6] (not to be confused with the Brent-Dekker method, see [6], chapters 3 and 4) is a widely used method for 1D optimization. It is based on golden section search and successive parabolic interpolations, and does not require evaluating any derivatives. This algorithm is guaranteed to converge to a local minimum with superlinear convergence of order at least 1.3247. Standard implementations of the YJ transformation, in particular the *scikit-learn* implementation [36], are based on the Brent minimization method to minimize the negative log-likelihood provided by Eq. (2).

Exponential search [3] is a dichotomic algorithm designed for unbounded search spaces. The idea is to first find bounds, and then to perform a classic binary search within these bounds. This algorithm can be used to find the minimum of convex differentiable functions with linear convergence, as explained in Appendix B. In this work, we build on exponential search to propose a federated version of the YJ transform, for two main reasons: (i) it is more numerically stable than Brent minimization, as shown in Section 3 and Figure 2, (ii), it may conveniently be adapted to a federated setting, as shown in Section 4, and (iii), this latter federated adaptation offers strong privacy guarantees, as shown by Proposition 4.1.

Secure Multiparty Computation As illustrated by various privacy gradient attacks [56, 54], sensitive information on the clients’ datasets can be leaked to the central server during an FL training. One way to mitigate this risk is to use Secure Multiparty Computation (SMC) protocols to hide individual contributions to the server. SMC enables one to evaluate functions with inputs distributed across different users without revealing intermediate results and is often based on secret sharing. SMC protocols tailored for ML use-cases have been recently proposed [12, 14, 34, 39, 48, 33, 49, 41]. These protocols are either designed to enhance the privacy of FL trainings, or to perform secure inference, i.e. to enable the evaluation of model trained privately on a server without revealing the data nor the model.

A popular FL algorithm relying on SMC is Secure Aggregation (SA) [4]. Schematically, in SA each client adds a random mask to their model update before sending it to the central server. These masks have been tailored in such a way that they all together sum to zero. Therefore, the central server cannot see the individual updates of the clients, but it can recover the sum of these updates by adding all the masked quantities sent from them.

More generally, an SMC routine schematically works as follows (we refer to Appendix D for further details). Let us consider the setting where K parties $k = 1, \dots, K$ want to compute $g = f(h^{(1)}, \dots, h^{(K)})$ for a known function f , where $(h^{(1)}, \dots, h^{(K)})$ denote private inputs. Each party k knows $h^{(k)}$ and is not willing to share it. During the first step, *secret sharing*, each party splits its private input $h^{(k)}$ into K secret shares $h_1^{(k)}, \dots, h_K^{(k)}$, and sends the shares $h_{k'}^{(k)}$ to the party k' . These secret shares are constructed in such a way that (i) knowing $h_{k'}^{(k)}$ does not provide any information on the value of $h^{(k)}$, and (ii) $h^{(k)}$ can be reconstructed from the vector $(h_1^{(k)}, \dots, h_K^{(k)})$. For simplicity, we denote $\llbracket h^{(k)} \rrbracket = (h_1^{(k)}, \dots, h_K^{(k)})$ the vector of share secrets. In a second step, *the computation*, each party k' computes the quantity denoted $g_{k'}$ using the secret shares they know along with intermediate quantities exchanged with the other parties. The way to compute $g_{k'}$ depends on f and on the SMC protocol that is used, and is chosen so that $g = f(h^{(1)}, \dots, h^{(K)})$ can be reconstructed from (g_1, \dots, g_K) . Said otherwise, $g_{k'}$ are secret shares of g : $\llbracket g \rrbracket = (g_1, \dots, g_K)$. Finally, during the *reveal* step, each party k reveals g_k to all other parties, and each party can reconstruct g from (g_1, \dots, g_K) .

Threat model In this work, we consider an honest-but-curious setting [35]. Neither the clients nor the server will deviate from the agreed protocol, but each party can potentially try to infer as much information as possible using data they see during the protocol. This setting is relevant for cross-silo FL, where participants are often large institutions whose reputation could be tarnished by a more malicious behaviour.

3 A novel method to optimize the Yeo-Johnson log-likelihood: EXPYJ

In this section, we leverage the convexity of the negative log-likelihood of the YJ transformation (see Proposition 3.1) to propose a new method to find the optimal λ_* using exponential search. While this method only offers linear convergence, compared to the super-linear convergence of Brent minimization method, we demonstrate two of its advantages: (i) it is more numerically stable, and (ii) it is easily amenable to an FL setting with strong privacy guarantees. The method proposed in this section is based on the following result.

Proposition 3.1. *The negative log-likelihood $\lambda \mapsto -\log \mathcal{L}_{\text{YJ}}(\lambda)$ (2) is strictly convex.*

Algorithm 1 EXPYJ

Input: data x_i , total data size n , number of steps t_{\max}
Initialize $\lambda_{t=0} \leftarrow 0$, $\lambda_{t=0}^+ \leftarrow \infty$, $\lambda_{t=0}^- \leftarrow -\infty$
Compute S_φ
for $t = 1$ **to** t_{\max}
 for $g \in \{\Psi(\lambda, \cdot), \Psi(\lambda, \cdot)^2, \partial_\lambda \Psi(\lambda, \cdot), \partial_\lambda \Psi(\lambda, \cdot)^2\}$
 Compute S_g
 end for
 $\Delta_t = \text{sgn} \left[nS_{\partial\Psi^2} - 2S_\Psi S_{\partial\Psi} - 2S_\varphi \left(S_{\Psi^2} - \frac{S_\Psi^2}{n} \right) \right]$
 $\lambda_t, \lambda_t^-, \lambda_t^+ \leftarrow \text{EXPUPDATE}(\lambda_{t-1}, \lambda_{t-1}^-, \lambda_{t-1}^+, \Delta_t)$
end for
 $\lambda_* \leftarrow \lambda_{t_{\max}}$
Compute $\mu_* = S_\Psi/n$ and $\sigma_*^2 = S_{\Psi^2}/n - \mu_*^2$
Output: The fitted triplet $(\lambda_*, \mu_*, \sigma_*^2)$

The proof of Proposition 3.1 builds upon the work of [26] which shows that the negative log-likelihood of the Box-Cox transformation [5] is convex. The complete proof is deferred to Appendix C.

The exponential YJ algorithm The pseudo-code of the proposed algorithm is presented in Algorithm 1, and relies on the exponential search presented in Algorithm 2 (cf Appendix B for more details on exponential search). An illustration of EXPYJ is shown in Figure 6 in Appendix B. Due to the strict convexity of the negative log-likelihood of the YJ transformation, we may perform the exponential search described in Section 2 and Appendix B. To do so, it is enough to obtain the sign of the derivative. Let $\partial_\lambda \Psi(\lambda, \cdot)^2 = 2\Psi(\lambda, \cdot)\partial_\lambda \Psi(\lambda, \cdot)$ and $\varphi(x) = \text{sgn}(x) + \log(|x| + 1)$. Further, for $g \in \{\Psi(\lambda, \cdot), \partial_\lambda \Psi(\lambda, \cdot), \Psi(\lambda, \cdot)^2, \partial_\lambda \Psi(\lambda, \cdot)^2, \varphi\}$, let us define $S_g \stackrel{\text{def}}{=} \sum_{i=1}^n g(x_i)$. The derivative of the log-likelihood is available in closed form (see Appendix A.3):

$$\partial_\lambda \log \mathcal{L}_{\text{YJ}} = \frac{n S_{\partial \Psi^2} - 2(S_\Psi S_{\partial \Psi})/n}{2 S_{\Psi^2} - S_\Psi^2/n} - S_\varphi.$$

Notice that $S_{\Psi^2} - S_\Psi^2/n$ can be expressed as a variance, hence is non-negative. We may therefore obtain $\text{sgn}[\partial_\lambda \log \mathcal{L}_{\text{YJ}}]$ while avoiding performing division by computing

$$\text{sgn}[\partial_\lambda \log \mathcal{L}_{\text{YJ}}] = \text{sgn}[n S_{\partial \Psi^2} - 2 S_\Psi S_{\partial \Psi} - 2 S_\varphi (S_{\Psi^2} - S_\Psi^2/n)]. \quad (3)$$

Avoiding this division is crucial to make the overall procedure more numerical stable, as explained below, and eases the use of SMC routines.

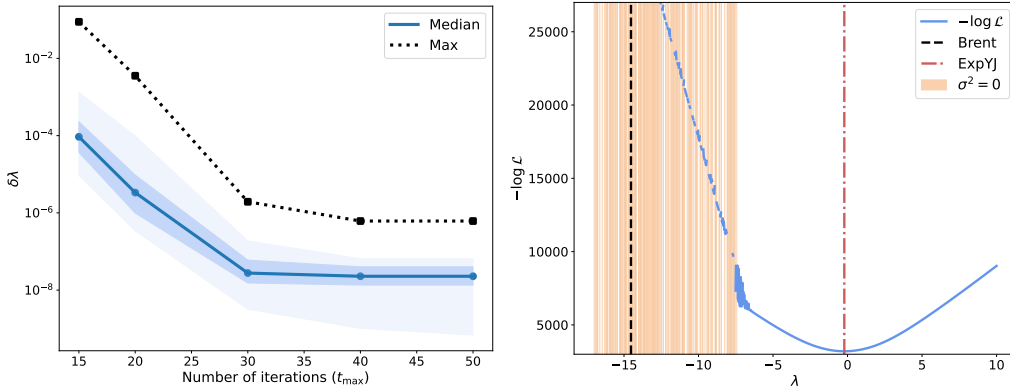


Figure 2: Comparison of EXPYJ and *scikit-learn*. **Left:** For each of the 106 features (see Appendix E.1), we compute the relative difference $\delta\lambda = |\lambda_{\text{EXPYJ}} - \lambda_{\text{sk}}|/|\lambda_{\text{sk}}|$ and plot its median, maximum and 25%-75% and 10%-90% percentiles across the 106 features. **Right:** Negative log-likelihood of the YJ transformation for the mean area of the cell of each sample of the *Breast Cancer* dataset. Full orange bars correspond to values of λ for which the likelihood computed using *scikit-learn* returns ∞ as $\sigma_\lambda^2(\{x_i\})$ is equal to 0 up to float-64 machine precision. Dotted lines correspond to the λ_* found using Brent minimization or EXPYJ with one client.

Accuracy of EXPYJ We check the accuracy of EXPYJ on the datasets presented in Appendix E.1. In particular, we compare the results provided by EXPYJ with the outputs of the *scikit-learn* algorithm based on Brent minimization.

For 2 of the 108 features present in the datasets, the *scikit-learn* implementation leads to numerical instabilities discussed hereafter. Therefore, we focus our comparison on the 106 remaining features, that we aggregated regardless of the dataset. Figure 2 reports the relative difference $\delta\lambda$ between the results obtained by EXPYJ and by the *scikit-learn* implementation as a function of the number of iteration t_{\max} (as defined in Algorithm 1). These results show that this relative difference is of order less than 10^{-6} when $t_{\max} = 40$.

Algorithm 2 EXPUPDATE

Input: $\lambda, \lambda^+, \lambda^-, \Delta \in \{-1, 1\}$

if $\Delta = 1$ **then**

$\lambda^- \leftarrow \lambda$

$\lambda \leftarrow (\lambda^+ + \lambda)/2$ **if** $\lambda^+ < \infty$

else $\lambda \leftarrow \max(2\lambda, 1)$

else

$\lambda^+ \leftarrow \lambda$

$\lambda \leftarrow (\lambda^- + \lambda)/2$ **if** $\lambda^- > -\infty$

else $\lambda \leftarrow \min(2\lambda, -1)$

end if

Output: Updated $\lambda, \lambda^+, \lambda^-$

Numerical stability of EXPYJ Our experiments demonstrate that EXPYJ is numerically more stable than Brent minimization. Indeed, for some values of λ and some datasets $\{x_i\}$, the transformation $\Psi(\lambda, \cdot)$ concentrates all data points in a small interval such that the values of $\Psi(\lambda, \{x_i\})$ are all equal up to machine precision. In that case, the log-likelihood is not well-defined and the term $\log \sigma_{\Psi_\lambda}^2$ takes the value $-\infty$, which prevents Brent minimization from converging. This phenomenon does not affect the EXPYJ routine as we do not compute directly the sign of $\partial_\lambda \mathcal{L} = \partial_\lambda \sigma_{\Psi_\lambda}^2 / \sigma_{\Psi_\lambda}^2 - \sum_i \varphi(x_i)$, but rather the sign of $\sigma_{\Psi_\lambda}^2 \partial_\lambda \mathcal{L} = -\partial_\lambda \sigma_{\Psi_\lambda}^2 - \sigma_{\Psi_\lambda}^2 \sum_i \varphi(x_i)$, see Eq. (3).

Figure 2 illustrates this in the case of a feature of the *Breast Cancer Dataset*. The λ_* returned by the Brent minimization method of *scikit-learn* is -14.53 while the minimizer of the negative log-likelihood found by the EXPYJ is -0.21 . In particular, Figure 2 shows the values of the negative log-likelihood as a function of λ computed using 64-bit float precision. The orange vertical full bands correspond to values for which $\sigma_{\Psi_\lambda}^2$ is zero within the machine precision, resulting to a negative log-likelihood of ∞ . This instability happens for 2 of the 108 features used in numerical experiments, where blindly applying the Brent-based YJ transformation leads to all data points collapsing to zero, while EXPYJ succeeds in transforming the data distributions to more Gaussian-like ones. Appendix E.4 shows that this issue also arises in other real-life datasets.

4 Applying the Yeo-Johnson transformation in FL

So far, we only considered the centralized setting, where data is accessible from a single server. Yet, as mentioned in Sections 1 and 2, many real-world situations require working with heterogeneous data split between different centers, and to take privacy constraints into account. When the data is split across centers $k = 1, \dots, K$ and the function to optimize is separable, i.e. of the form $\mathcal{F}(\lambda) = \sum_{k=1}^K f_k(\lambda)$ where each f_k can be computed from data present in the center k exclusively, Federated Learning techniques were recently proposed. In short, they consist in repeatedly performing a few rounds of local optimization in each center, before aggregating local parameters in the server. We refer to [23] for an overview of recent advances in FL. In our case, however, the YJ negative log-likelihood (2) is not separable, due to the log-variance term. Indeed, turning the variance into a separable term would require sharing the global YJ mean μ_λ to all centers at each iteration. Compared to the method we propose in this section, this would lead to more privacy leakage.

We now introduce SECUREFEDYJ, a secure federated algorithm that builds upon EXPYJ to apply YJ transformations. This algorithm satisfies the two following properties: (i) it is *pooled-equivalent*, i.e. it yields the same results as if the data were freely accessible from a single server, and (ii) it leaks as little information as possible about the underlying datasets, as shown by Proposition 4.1. Finally, it converges in a limited number of iterations, thanks to the linear convergence of the underlying exponential search.

SECUREFEDYJ SECUREFEDYJ is a federated adaptation of EXPYJ presented in Section 3 to find the best parameters $(\lambda_*, \mu_*, \sigma_*^2)$ of the YJ transformation when training datasets are split across different clients. It relies on SMC to ensure that only the final triplet $(\lambda_*, \mu_*, \sigma_*^2)$ fitted on the training datasets is revealed, without leaking any other information apart from the overall total number of training samples n . Indeed, at each intermediate step, only the sign of $\partial_\lambda \log \mathcal{L}_{YJ}$ is revealed, and the mean and variance of the transformed data is only revealed at the last step. The pseudo-code of the resulting algorithm is presented in Algorithm 3, and relies on the exponential search presented in Algorithm 2. A functional representation of SECUREFEDYJ is displayed Figure 7.

In Algorithm 3, we label the clients by $k = 1, \dots, K$ and each client k holds data $\{x_{k,i} : i = 1, \dots, n_k\}$. We suppose that the total number of samples $n = \sum_{k=1}^K n_k$ is public and shared to all clients. For a given function g , we denote $S_{k,g}$ the sum $S_{k,g} \stackrel{\text{def}}{=} \sum_{i=1}^{n_k} g(x_{k,i})$. As introduced in Section 2, we use double brackets $\llbracket \cdot \rrbracket$ to indicate an SMC secret shared across the clients (see Appendix D for more details).

Privacy leakage In Proposition 4.1 we show that Algorithm 3 only reveals information already contained in the fitted triplet $(\lambda_*, \mu_*, \sigma_*^2)$. In comparison, turning the YJ negative log-likelihood (2) into a log-separable function before using off-the-shelf FL methods would require sharing μ and its gradient and centrally computing σ^2 for intermediate values of λ at each iteration. This could potentially lead to uncontrolled privacy leakage.

Algorithm 3 SECUREFEDYJ

Input: Data $\{x_{k,i}\}$, total data size n , number of steps t_{\max}

Notations: $[\![\cdot]\!]$ indicates a SMC secret shared across the clients. Any operation such as $[\![\cdot]\!] = f([\![\cdot]\!], [\![\cdot]\!], \dots)$ where f can be the sum, product, or the sign, designs an SMC routine across the clients as described in Appendix D.5.

Initialize $\lambda_{t=0} \leftarrow 0$, $\lambda^+ \leftarrow \infty$, $\lambda^- \leftarrow -\infty$ independently on each client

Clients compute in SMC $[\![S_\varphi]\!] = \sum_k [\![S_{k,\varphi}]\!]$

for $t = 1$ **to** t_{\max}

for $g \in \{\Psi(\lambda, \cdot), \Psi(\lambda, \cdot)^2, \partial_\lambda \Psi(\lambda, \cdot), \partial \Psi(\lambda, \cdot)^2\}$

 Clients compute in SMC $[\![S_g]\!] = \sum_k [\![S_{k,g}]\!]$,

end for

 Clients compute in SMC $[\![\Delta_t]\!] = \text{sgn}[n[\![S_{\partial \Psi^2}]\!] - 2[\![S_\Psi]\!][\![S_{\partial \Psi}]\!] - 2[\![S_\varphi]\!](\![S_{\Psi^2}\!] - \![S_\Psi]^2/n)]$

 Clients reveal Δ_t

$\lambda_t, \lambda_t^-, \lambda_t^+ \leftarrow \text{EXPUPDATE}(\lambda_{t-1}, \lambda_{t-1}^-, \lambda_{t-1}^+, \Delta_t)$ independently on each client

end for

$\lambda_* \leftarrow \lambda_{t_{\max}}$

Clients compute in SMC $[\![\mu]\!] = \sum_k [\![S_{k,\Psi}]\!]/n$ and $[\![\sigma^2]\!] = \sum_k [\![S_{k,\Psi^2}]\!]/n - [\![\mu]^2]$

Clients reveal $\mu_* \leftarrow \mu$ and $\sigma_*^2 \leftarrow \sigma^2$

Output: The fitted triplet $(\lambda_*, \mu_*, \sigma_*^2)$

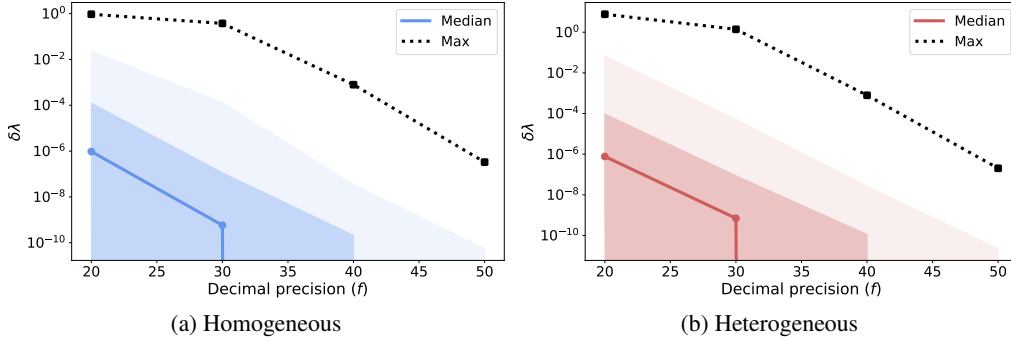


Figure 3: Comparison of SECUREFEDYJ and EXPYJ for various fixed-point floating precisions f used in SMC, with $l = f + 50$ and $t_{\max} = 40$. The data is distributed across 10 clients, either randomly (homogeneous, *left*), or per decile (heterogeneous, *right*, i.e. each client gets one decile of the data). We report the maximum, median, 25%-75% and 10%-90% percentiles of the relative error $\delta\lambda = |\lambda_{\text{SECUREFEDYJ}} - \lambda_{\text{EXPYJ}}|/|\lambda_{\text{EXPYJ}}|$ across the 108 features described in Appendix E.1.

Proposition 4.1. *The fitted parameter λ_* contains all the information revealed during the intermediate steps of SECUREFEDYJ. More precisely, there exists a deterministic function \mathcal{F} such that for any set of datasets $\{x_{k,i}\}$, if $\lambda_*(\{x_{k,i}\})$ is the result of SECUREFEDYJ on $\{x_{k,i}\}$, then $\{\lambda_t, \lambda_t^+, \lambda_t^-, \Delta_t\}_{t=1, \dots, t_{\max}} = \mathcal{F}[\lambda_*(\{x_{k,i}\})]$*

Proof. This proposition comes from the fact that all gradient signs Δ_t revealed during the algorithm can be retrospectively inferred from λ_* . Indeed, $\partial_\lambda \log \mathcal{L}_{\text{YJ}} < 0$ for $\lambda > \lambda_*$ and $\partial_\lambda \log \mathcal{L}_{\text{YJ}} > 0$ for $\lambda < \lambda_*$. Besides, the successive values of λ_t explored at each step t can be deterministically inferred from the initial value $\lambda_{t=0}$ and the final fitted value λ_* . We construct such a function \mathcal{F} and numerical verify this proposition in Appendix F. ■

Performance of SECUREFEDYJ We implement SECUREFEDYJ in Python, using the MPyC library [42] based on Shamir Secret Sharing [44]. We refer to Appendix D for more details on our implementation. To represent signed real-valued numbers in an SMC protocol, we use a fixed-point representation (see Appendix D.2) using l bits, among which f bits are used for the decimal parts. This means that we consider floats ranging from -2^{l-f} to 2^{l-f} and that we have an absolute precision of 2^{-f} in our computations.

In order to ensure the accuracy of SECUREFEDYJ results, we need to make sure that l and f are large enough. Figure 3 shows the accuracy of SECUREFEDYJ when compared to EXPYJ for various values of f . According to these numerical experiments, taking $f = 50$ and $l = 100$ provides reasonably accurate results. Moreover, by construction, the outputs of SECUREFEDYJ do not depend on how the data is split across the clients, up to rounding numerical errors. Therefore this algorithm is resilient to data heterogeneity, as long as the numerical decimal precision f is large enough, as shown in Figure 3.

Performing SECUREFEDYJ with $t_{\max} = 40$ takes 726 rounds of communication (see Appendix D.6). During these communication rounds, each client sends overall about 8 Mb per feature to every other client (see also Appendix D.6). SECUREFEDYJ can be applied independently and in parallel to each feature. Therefore, the overall number of rounds does not depend on the number of features being considered, and the communication costs grow proportionally to the number of features. In a realistic cross-silo FL setting as described in [19], the bandwidth of the network is 1 Gb per second with a delay of 20 ms between every two clients. In this context, the execution of SECUREFEDYJ with $t_{\max} = 40$ on p features would take about $726 \times 20 \text{ ms} \simeq 15 \text{ s}$ due to the communication overhead, in addition to $p \times 8 \text{ Mb}/1 \text{ Gbps} \simeq 8p \text{ ms}$ due to the bandwidth. This shows that SECUREFEDYJ is indeed a viable algorithm in a real-world scenario.

As pointed out in Appendix B, the binary search in the exponential search can be replaced by a k -ary search. In such a setting, the sign of the negative log-likelihood of the YJ transformation is computed for $k - 1$ different values of λ at each round. Such a modification would reduce the number of communication rounds required to obtain a given accuracy, while increasing the size of the data exchanged over the network at each round.

5 Applications

Genomic data: TCGA We start by showing the benefits of YJ preprocessing in survival analysis experiments on lung (LUAD+LUSC), pancreas (PAAD), and colorectal (CRC) cancers. Given gene expression raw counts (features) and censored survival data (responses) from patients having either of those three cancers, we aim to fit a Cox Proportional Hazards (CoxPH) model [10] with the highest possible concordance index (C-index) [25], which measures how well patients are ranked with respect to their survival times. We refer to [25] for a more thorough introduction to survival analysis. In Figure 4, we compare three different preprocessing methods: (i) whitening, (ii) log normalization, and (iii) YJ, each followed by a PCA dimensionality reduction step. More precisely, whitening (i) consists in centering and reducing to unit variance the total read counts of all genes across all samples, log normalization consists in applying $u \mapsto \log(1 + u)$ to raw read counts before applying global whitening, and YJ is a global YJ transform on the total read counts. We then evaluate each strategy using 5-fold cross-validation with 5 different seeds. We refer to Appendix E.2 for experimental details. While this experiment is performed in a pooled environment, note that, importantly, each step has a federated pooled-equivalent version: apart from the proposed SECUREFEDYJ for YJ, see e.g. [21] for PCA, and Webdisco [31] for Cox model fitting. This simplified setting allows us to understand the importance of the Yeo-Johnson transformation in an ideal setting, independently of other potential downstream federated learning artifacts.

In Figure 4, we see that YJ is better or on par with the best method for each cancer: YJ improves prediction results for colorectal cancer, while yielding results which are on par with the best results for lung and pancreas cancers, with a smaller variance.

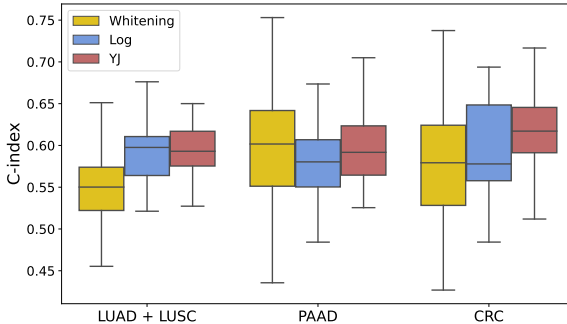


Figure 4: Cross-validation survival analysis performance (higher is better) of a CoxPH model with different normalization methods. The YJ transformation yields either a better or on par performance, and further stabilizes results compared to other approaches.

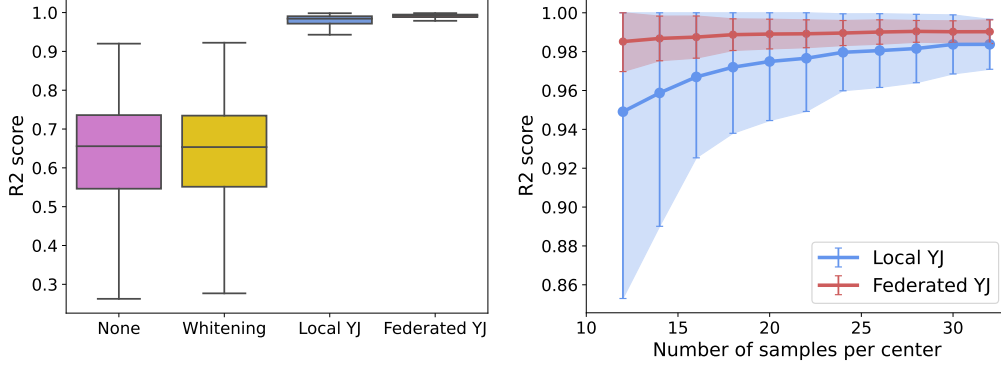


Figure 5: Comparison of different preprocessing methods for linear regression on synthetic federated data. **Left:** performance with 200 samples (20 on each of the 10 centers) on 1000 independent draws, showing the interest of using YJ preprocessing. The R2 score of the models are computed on another dataset of 200 samples not seen during the training. **Right:** Comparison of local and federated YJ over 1000 independent draws. In local YJ, a single center is randomly chosen to fit λ , which is then shared with other centers, to ensure that the same transformation is applied everywhere. Full lines correspond to the means, error bars to \pm std of the R2 scores of the model on an unseen test dataset.

Synthetic data We show how applying YJ may help improving performance compared to no or basic preprocessing, and how SECUREFEDYJ yields improvements compared to local YJ transforms in federated linear regression. To do so, we generate covariates \tilde{X} and responses y as

$$\begin{aligned} \tilde{X} &= (\exp(x_1), \exp(x_2 + 2), \sigma(x_3)) \text{ with } X = (x_1, x_2, x_3) \sim \mathcal{N}(0, \mathbf{I}_3), \\ y &= \beta^T X + \varepsilon \text{ with } \varepsilon \sim \mathcal{N}(0, 0.1), \end{aligned} \quad (4)$$

where $\sigma(\cdot)$ is the sigmoid function and $\beta = (-1.3, 2.4, 0.87)$ was randomly chosen. The goal is then to fit a linear model from i.i.d. samples $(\tilde{X}_i, y_i), i = 1, \dots, n$ following (4), after an optional preprocessing step. Similarly to the previous example, we simulate a cross-device FL setting only for the preprocessing steps, and the linear model is then fitted in a pooled setting for simplicity. All the details of the numerical experiments are provided in Appendix E.3. We suppose that the samples $(\tilde{X}_i, y_i), i = 1, \dots, n$ are homogeneously split across 10 centers. The responses y_i have a highly nonlinear dependency on the covariates \tilde{X}_i , but depend linearly on the X_i 's (up to Gaussian noise), which are not observed. Hence, we expect that applying a suitable preprocessing step before training a linear model will transform back the \tilde{X}_i 's into the normally-distributed X_i 's and lead to a high performance, compared to no transformation. The results of our experiments are summarized in Figure 5. The left figure shows that the YJ transformation is indeed capable of roughly inverting the \tilde{X}_i 's into the X_i 's, yielding a major improvement compared to no preprocessing or standard centering and reduction to unit variance. Besides, the right figure shows that even in this homogeneous setting where the data is i.i.d. across centers, using a federated version of YJ compared to a local version of YJ leads to better average performance, and reduced variance.

6 Conclusion

Summary of our contributions In this work, we introduce SECUREFEDYJ, a method to fit a YJ transformation on data shared by different clients in a cross-silo setting. SECUREFEDYJ is an SMC version of its pooled equivalent EXPYJ which builds upon the convexity of the negative log-likelihood of the YJ transformation, a novel result introduced by this work, and on the fact that the sign of its derivative can be computed in a stable way. We show that SECUREFEDYJ has the same accuracy as a standard YJ transformation on pooled data. In particular, the results do not depend on how the data is split across the clients, making SECUREFEDYJ resilient to data heterogeneity. Besides, the quantities disclosed by SECUREFEDYJ during the training to the central server do not leak any other information than what is contained in the final parameters $(\mu_*, \lambda_*, \sigma_*^2)$.

Limitations and future work While Brent minimization has a super-linear convergence, our approach only has a linear convergence, as it relies on exponential search. This can be an issue if the communication costs between the clients and the server are high. Acceleration could be achieved by either adapting Brent minimization to a cross-silo setting, or applying a second-order method. We leave the development of a faster SMC methods using either of those two approaches to future work.

Another limitation is that even if our approach reveals only information that would be contained in the final fitted parameters, such parameters themselves might leak information about individual samples, as our approach is not differentially private (DP) [16]. By adding Gaussian or Laplacian noise to each sample’s features when computing the S_g terms one could, in principle, make the resulting algorithm DP [1]. However it is unclear to what extent the noise would impact the final accuracy of the method.

Finally, we only consider an *honest-but-curious* setting. We do not explore the threat of a malicious participant that would purposely deviate from the protocol to either gain more information or to jeopardize the convergence. We leave this investigation to future work.

Acknowledgement

The authors would like to thank the four anonymous reviewers, as well as the anonymous area chair reviewer for their relevant comments and ideas which significantly improved the paper.

References

- [1] Martin Abadi, Andy Chu, Ian Goodfellow, H Brendan McMahan, Ilya Mironov, Kunal Talwar, and Li Zhang. Deep learning with differential privacy. In *Proceedings of the 2016 ACM SIGSAC Conference on Computer and Communications Security*, pages 308–318, 2016.
- [2] Mathieu Andreux, Jean Ogier du Terrail, Constance Beguier, and Eric W Tramel. Siloed federated learning for multi-centric histopathology datasets. In *Domain Adaptation and Representation Transfer, and Distributed and Collaborative Learning*, pages 129–139. Springer, 2020.
- [3] Jon Louis Bentley and Andrew Chi-Chih Yao. An almost optimal algorithm for unbounded searching. *Information processing letters*, 5(SLAC-PUB-1679), 1976.
- [4] Keith Bonawitz, Vladimir Ivanov, Ben Kreuter, Antonio Marcedone, H Brendan McMahan, Sarvar Patel, Daniel Ramage, Aaron Segal, and Karn Seth. Practical secure aggregation for privacy-preserving machine learning. In *Proceedings of the 2017 ACM SIGSAC Conference on Computer and Communications Security*, pages 1175–1191, 2017.
- [5] George EP Box and David R Cox. An analysis of transformations. *Journal of the Royal Statistical Society: Series B (Methodological)*, 26(2):211–243, 1964.
- [6] Richard P Brent. *Algorithms for Minimization Without Derivatives*. Prentice Hall, 1973.
- [7] Franziska S Brunner, Paul Schmid-Hempel, and Seth M Barribeau. Immune gene expression in *bombus terrestris*: signatures of infection despite strong variation among populations, colonies, and sister workers. *PloS one*, 8(7):e68181, 2013.
- [8] Octavian Catrina and Amitabh Saxena. Secure computation with fixed-point numbers. In *International Conference on Financial Cryptography and Data Security*, pages 35–50. Springer, 2010.
- [9] Li-Chu Chien. A rank-based normalization method with the fully adjusted full-stage procedure in genetic association studies. *PloS one*, 15(6):e0233847, 2020.
- [10] David R Cox. Regression models and life-tables. *Journal of the Royal Statistical Society: Series B (Methodological)*, 34(2):187–202, 1972.
- [11] Ivan Damgård, Martin Geisler, Mikkel Krøigaard, and Jesper Buus Nielsen. Asynchronous multiparty computation: Theory and implementation. In *International workshop on public key cryptography*, pages 160–179. Springer, 2009.

- [12] Ivan Damgård, Marcel Keller, Enrique Larraia, Valerio Pastro, Peter Scholl, and Nigel P Smart. Practical covertly secure MPC for dishonest majority—or: breaking the SPDZ limits. In *European Symposium on Research in Computer Security*, pages 1–18. Springer, 2013.
- [13] Thiago Alexandre das Neves Almeida, Luís Cruz, Eduardo Barata, and Isabel-María García-Sánchez. Economic growth and environmental impacts: An analysis based on a composite index of environmental damage. *Ecological Indicators*, 76:119–130, 2017.
- [14] Daniel Demmler, Thomas Schneider, and Michael Zohner. ABY-A framework for efficient mixed-protocol secure two-party computation. In *NDSS*, 2015.
- [15] Dheeru Dua and Casey Graff. UCI machine learning repository, 2017. URL <http://archive.ics.uci.edu/ml>.
- [16] Cynthia Dwork. Differential privacy. In *International Colloquium on Automata, Languages, and Programming*, pages 1–12. Springer, 2006.
- [17] Daniel Escudero, Satrajit Ghosh, Marcel Keller, Rahul Rachuri, and Peter Scholl. Improved primitives for mpc over mixed arithmetic-binary circuits. In *Annual International Cryptology conference*, pages 823–852. Springer, 2020.
- [18] Ronald A Fisher. The use of multiple measurements in taxonomic problems. *Annals of eugenics*, 7(2):179–188, 1936.
- [19] David Froelicher, Juan R Troncoso-Pastoriza, Jean Louis Raisaro, Michel Cuendet, Joao Sa Sousa, Jacques Fellay, and Jean-Pierre Hubaux. Truly privacy-preserving federated analytics for precision medicine with multiparty homomorphic encryption. *Nature Communications*, 12(1):5910, 2021.
- [20] Ian Goodfellow, David Warde-Farley, Mehdi Mirza, Aaron Courville, and Yoshua Bengio. Maxout networks. In *International Conference on Machine Learning*, pages 1319–1327. PMLR, 2013.
- [21] Andreas Grammenos, Rodrigo Mendoza Smith, Jon Crowcroft, and Cecilia Mascolo. Federated principal component analysis. In H. Larochelle, M. Ranzato, R. Hadsell, M.F. Balcan, and H. Lin, editors, *Advances in Neural Information Processing Systems*, volume 33, pages 6453–6464. Curran Associates, Inc., 2020.
- [22] Ian Jolliffe. Principal component analysis. *Encyclopedia of statistics in behavioral science*, 2005.
- [23] Peter Kairouz, H Brendan McMahan, Brendan Avent, Aurélien Bellet, Mehdi Bennis, Arjun Nitin Bhagoji, Kallista Bonawitz, Zachary Charles, Graham Cormode, Rachel Cummings, et al. Advances and open problems in federated learning. *Foundations and Trends® in Machine Learning*, 14(1–2):1–210, 2021.
- [24] Sai Praneeth Karimireddy, Satyen Kale, Mehryar Mohri, Sashank Reddi, Sebastian Stich, and Ananda Theertha Suresh. Scaffold: Stochastic controlled averaging for federated learning. In *International Conference on Machine Learning*, pages 5132–5143. PMLR, 2020.
- [25] David G Kleinbaum and Mitchel Klein. *Survival analysis*, volume 3. Springer, 2010.
- [26] Elies Kouider and Hanfeng Chen. Concavity of Box-Cox log-likelihood function. *Statistics and probability letters*, 25(2):171–175, 1995.
- [27] Alex Krizhevsky, Geoffrey Hinton, et al. Learning multiple layers of features from tiny images. 2009.
- [28] Tian Li, Anit Kumar Sahu, Ameet Talwalkar, and Virginia Smith. Federated learning: Challenges, methods, and future directions. *IEEE Signal Processing Magazine*, 37(3):50–60, 2020.
- [29] Tian Li, Anit Kumar Sahu, Manzil Zaheer, Maziar Sanjabi, Ameet Talwalkar, and Virginia Smith. Federated optimization in heterogeneous networks. *Proceedings of Machine Learning and Systems*, 2:429–450, 2020.

- [30] Thomas Lorünser and Florian Wohner. Performance comparison of two generic MPC-frameworks with symmetric ciphers. In *ICETE (2)*, pages 587–594, 2020.
- [31] Chia-Lun Lu, Shuang Wang, Zhanglong Ji, Yuan Wu, Li Xiong, Xiaoqian Jiang, and Lucila Ohno-Machado. Webdisco: a web service for distributed cox model learning without patient-level data sharing. *Journal of the American Medical Informatics Association*, 22(6):1212–1219, 2015.
- [32] Brendan McMahan, Eider Moore, Daniel Ramage, Seth Hampson, and Blaise Aguera y Arcas. Communication-efficient learning of deep networks from decentralized data. In *Artificial intelligence and statistics*, pages 1273–1282. PMLR, 2017.
- [33] Payman Mohassel and Peter Rindal. ABY3: A mixed protocol framework for machine learning. In *Proceedings of the 2018 ACM SIGSAC Conference on Computer and Communications Security*, pages 35–52, 2018.
- [34] Payman Mohassel and Yupeng Zhang. SecureML: A system for scalable privacy-preserving machine learning. In *2017 IEEE symposium on security and privacy (SP)*, pages 19–38. IEEE, 2017.
- [35] Andrew Paverd, Andrew Martin, and Ian Brown. Modelling and automatically analysing privacy properties for honest-but-curious adversaries. *Tech. Rep.*, 2014.
- [36] F. Pedregosa, G. Varoquaux, A. Gramfort, V. Michel, B. Thirion, O. Grisel, M. Blondel, P. Prettenhofer, R. Weiss, V. Dubourg, J. Vanderplas, A. Passos, D. Cournapeau, M. Brucher, M. Perrot, and E. Duchesnay. Scikit-learn: Machine learning in Python. *Journal of Machine Learning Research*, 12:2825–2830, 2011.
- [37] Tord Ingolf Reistad. A general framework for multiparty computations. 2012.
- [38] Tord Ingolf Reistad and Tomas Toft. Secret sharing comparison by transformation and rotation. In *International Conference on Information Theoretic Security*, pages 169–180. Springer, 2007.
- [39] M Sadegh Riazi, Christian Weinert, Oleksandr Tkachenko, Ebrahim M Songhori, Thomas Schneider, and Farinaz Koushanfar. Chameleon: A hybrid secure computation framework for machine learning applications. In *Proceedings of the 2018 on Asia Conference on Computer and Communications Security*, pages 707–721, 2018.
- [40] Nicola Rieke, Jonny Hancox, Wenqi Li, Fausto Milletari, Holger R Roth, Shadi Albarqouni, Spyridon Bakas, Mathieu N Galtier, Bennett A Landman, Klaus Maier-Hein, et al. The future of digital health with federated learning. *NPJ digital medicine*, 3(1):1–7, 2020.
- [41] Théo Ryffel, Pierre Tholoniati, David Pointcheval, and Francis Bach. AriaNN: Low-interaction privacy-preserving deep learning via function secret sharing. *Proceedings on Privacy Enhancing Technologies*, 1:291–316, 2022.
- [42] Berry Schoenmakers. MPyC—python package for secure multiparty computation. In *Workshop on the Theory and Practice of MPC.*, 2018. URL <https://github.com/lschoe/mpyc>.
- [43] Muhammad Shafiq-ul Hassan, Geoffrey G Zhang, Kujtim Latifi, Ghanim Ullah, Dylan C Hunt, Yoganand Balagurunathan, Mahmoud Abraham Abdalah, Matthew B Schabath, Dmitry G Goldgof, Dennis Mackin, et al. Intrinsic dependencies of CT radiomic features on voxel size and number of gray levels. *Medical physics*, 44(3):1050–1062, 2017.
- [44] Adi Shamir. How to share a secret. *Communications of the ACM*, 22(11):612–613, 1979.
- [45] Reza Shokri and Vitaly Shmatikov. Privacy-preserving deep learning. In *Proceedings of the 22nd ACM SIGSAC Conference on Computer and Communications Security*, pages 1310–1321, 2015.
- [46] Jost Tobias Springenberg, Alexey Dosovitskiy, Thomas Brox, and Martin Riedmiller. Striving for simplicity: The all convolutional net. *arXiv preprint arXiv:1412.6806*, 2014.

- [47] David Tellez, Geert Litjens, Péter Bándi, Wouter Bulten, John-Melle Bokhorst, Francesco Ciompi, and Jeroen van der Laak. Quantifying the effects of data augmentation and stain color normalization in convolutional neural networks for computational pathology. *Medical image analysis*, 58:101544, 2019.
- [48] Sameer Wagh, Divya Gupta, and Nishanth Chandran. SecureNN: Efficient and private neural network training. *IACR Cryptol. ePrint Arch.*, 2018:442, 2018.
- [49] Sameer Wagh, Shruti Tople, Fabrice Benhamouda, Eyal Kushilevitz, Prateek Mittal, and Tal Rabin. FALCON: Honest-majority maliciously secure framework for private deep learning. *arXiv preprint arXiv:2004.02229*, 2020.
- [50] QJ Wang and DE Robertson. Multisite probabilistic forecasting of seasonal flows for streams with zero value occurrences. *Water Resources Research*, 47(2), 2011.
- [51] QJ Wang, Andrew Schepen, and David E Robertson. Merging seasonal rainfall forecasts from multiple statistical models through bayesian model averaging. *Journal of Climate*, 25(16): 5524–5537, 2012.
- [52] In-Kwon Yeo and Richard A Johnson. A new family of power transformations to improve normality or symmetry. *Biometrika*, 87(4):954–959, 2000.
- [53] Lina Zhang, Bizheng Wang, and Qingcun Zeng. Impact of the Madden–Julian oscillation on summer rainfall in southeast China. *Journal of Climate*, 22(2):201–216, 2009.
- [54] Bo Zhao, Konda Reddy Mopuri, and Hakan Bilen. iDLG: Improved deep leakage from gradients. *arXiv preprint arXiv:2001.02610*, 2020.
- [55] Wenting Zheng, Raluca Ada Popa, Joseph E Gonzalez, and Ion Stoica. Helen: Maliciously secure cooperative learning for linear models. In *2019 IEEE Symposium on Security and Privacy (SP)*, pages 724–738. IEEE, 2019.
- [56] Ligeng Zhu, Zhijian Liu, and Song Han. Deep leakage from gradients. In *Advances in Neural Information Processing Systems*, volume 32. Curran Associates, Inc., 2019.
- [57] Olga Zolotareva, Reza Nasirigerdeh, Julian Matschinske, Reihaneh Torkzadehmahani, Mohammad Bakhtiari, Tobias Frisch, Julian Späth, David B Blumenthal, Amir Abbasinejad, Paolo Tieri, et al. Flimma: a federated and privacy-aware tool for differential gene expression analysis. *Genome biology*, 22(1):1–26, 2021.
- [58] Isabella Zwiener, Barbara Frisch, and Harald Binder. Transforming RNA-Seq data to improve the performance of prognostic gene signatures. *PloS one*, 9(1):e85150, 2014.

Checklist

1. For all authors...
 - (a) Do the main claims made in the abstract and introduction accurately reflect the paper’s contributions and scope? [\[Yes\]](#)
 - (b) Did you describe the limitations of your work? [\[Yes\]](#) We described them in Section 6
 - (c) Did you discuss any potential negative societal impacts of your work? [\[N/A\]](#)
 - (d) Have you read the ethics review guidelines and ensured that your paper conforms to them? [\[Yes\]](#)
2. If you are including theoretical results...
 - (a) Did you state the full set of assumptions of all theoretical results? [\[Yes\]](#)
 - (b) Did you include complete proofs of all theoretical results? [\[Yes\]](#) The full proof of the main theoretical results, i.e. the convexity of the Yeo-Johnson negative log-likelihood (Proposition 3.1) is provided in Appendix C.
3. If you ran experiments...

- (a) Did you include the code, data, and instructions needed to reproduce the main experimental results (either in the supplemental material or as a URL)? [No] The code of the experiments is not provided, but a detailed pseudo-code of the newly proposed algorithms are provided.
 - (b) Did you specify all the training details (e.g., data splits, hyperparameters, how they were chosen)? [Yes] We specified all the hyperparameters and the details of the numerical experiment in Appendix E.
 - (c) Did you report error bars (e.g., with respect to the random seed after running experiments multiple times)? [Yes] Standard deviations or quantiles of the results with respect to the seed are provided (cf plots)
 - (d) Did you include the total amount of compute and the type of resources used (e.g., type of GPUs, internal cluster, or cloud provider)? [No] The experiment are not heavy and run easily on a personal computer, on a CPU
4. If you are using existing assets (e.g., code, data, models) or curating/releasing new assets...
- (a) If your work uses existing assets, did you cite the creators? [Yes] The datasets used are open datasets available online and are systematically cited.
 - (b) Did you mention the license of the assets? [Yes] The licence of the datasets used are provided in Appendix E.1
 - (c) Did you include any new assets either in the supplemental material or as a URL? [No]
 - (d) Did you discuss whether and how consent was obtained from people whose data you're using/curating? [N/A] We are using open datasets available online. The genomic dataset from TCGA have been previously anonymised by its creator before publication
 - (e) Did you discuss whether the data you are using/curating contains personally identifiable information or offensive content? [N/A]
5. If you used crowdsourcing or conducted research with human subjects...
- (a) Did you include the full text of instructions given to participants and screenshots, if applicable? [N/A]
 - (b) Did you describe any potential participant risks, with links to Institutional Review Board (IRB) approvals, if applicable? [N/A]
 - (c) Did you include the estimated hourly wage paid to participants and the total amount spent on participant compensation? [N/A]

A Additional properties of the Yeo-Johnson transformation

A.1 Derivation of the Yeo-Johnson log-likelihood

Using the change of variables rule, the probability to draw a set of points $\{x_i\}$ such that $\{\Psi(\lambda, x_i)\}$ follows a Gaussian distribution of mean μ and variance σ^2 is given by:

$$\mathbb{P}(\{x_i\}|\lambda, \mu, \sigma) = \mathbb{P}(\{\Psi_\lambda(\lambda, x_i)\}|\lambda, \mu, \sigma) * \det J[\{x_i\}, \Psi(\lambda, x_i)] \quad (5)$$

where $\det J[x_i, \Psi(\lambda, x_i)]$ is the determinant of the Jacobian matrix $J[\{x_i\}, \{\Psi(\lambda, x_i)\}]$ defined as:

$$J[\{x_i\}, \{\Psi(\lambda, x_i)\}]_{ab} = \frac{\partial \Psi(\lambda, x_a)}{\partial x_b}$$

This matrix is diagonal and each term of its diagonal can be computed using Eq. (1). For each value of λ and x_i , these diagonal terms can be re-written as $\exp[(\lambda - 1) \operatorname{sgn}(x_i) \log(|x_i| + 1)]$. The term $\mathbb{P}(\{\Psi_\lambda(\lambda, x_i)\}|\lambda, \mu, \sigma)$ is equal to:

$$\mathbb{P}(\{\Psi_\lambda(\lambda, x_i)\}|\lambda, \mu, \sigma) = \prod_i \frac{1}{\sigma\sqrt{2\pi}} \exp\left[-\frac{(x_i - \mu)^2}{2\sigma^2}\right]$$

By taking the logarithm of Eq. (5), we obtain the log-likelihood provided in Section 1 and originally derived on [52].

A.2 Relationship with the Box-Cox transformation

The Box-Cox transformation [5] works similarly to the YJ transformation, but only applies to strictly positive data. The Box-Cox transformation is based on a function $\Phi(\lambda, \cdot)$ parametrized by λ and defined for $x > 0$ as:

$$\Phi(\lambda, x) = \begin{cases} \frac{x^\lambda - 1}{\lambda}, & \text{if } \lambda \neq 0, \\ \ln(x), & \text{if } \lambda = 0. \end{cases}$$

It is straightforward to check that for any $\lambda \in \mathbb{R}$ the YJ transformation Ψ and the Box-Cox transformation Φ are related by the following equations:

$$\Psi(\lambda, x) = \begin{cases} \Phi(\lambda, x + 1) & \text{if } x \geq 0, \\ -\Phi(2 - \lambda, 1 - x) & \text{if } x < 0. \end{cases}$$

A.3 Analytical formulae for the derivatives of the Yeo-Johnson transformation

The YJ function is infinitely differentiable with respect to both of its variables (x and λ). Here are its successive derivatives with respect to λ :

$$\partial_\lambda^k \Psi(\lambda, x) = \begin{cases} [(x + 1)^\lambda [\ln(x + 1)]^k - k \partial_\lambda^{k-1} \Psi(\lambda, x)] / \lambda, & \text{if } x \geq 0, \lambda \neq 0, \\ \ln(x + 1)^{k+1} / (k + 1), & \text{if } x \geq 0, \lambda = 0, \\ ([-x + 1]^{2-\lambda} [\ln(-x + 1)]^k + k \partial_\lambda^{k-1} \Psi(\lambda, x)) / (2 - \lambda), & \text{if } x < 0, \lambda \neq 2, \\ (-\ln(-x + 1))^{k+1} / (k + 1), & \text{if } x < 0, \lambda = 2. \end{cases}$$

B Background on exponential search

Exponential search [3] is a method to look for an element in an unbounded sorted array. The idea is to first find bounds on the array such that the element is contained within such bounds, and then perform a classic binary search inside these bounds. Let us consider the task of finding the smallest element u_{i_0} greater than a threshold C in an unbounded sorted array $\{u_i\}_{i \in \mathbb{N}^*}$. The exponential search iteratively looks at u_i for $i \in \{1, 2, 2^2, 2^4, \dots\}$ until it finds a i_{\max} such that $u_{i_{\max}} \geq C$. This takes $\log_2(i_{\max})$ steps. Then it performs a binary search between $i = i_{\max}/2$ and $i = i_{\max}$, which also takes $\log_2(i_{\max}/2)$ steps.

If $f(s)$ is a strictly increasing function of s taking both positive and negative values, one can adapt the exponential search to find the root s_0 of f . The first step is to find an upper and a lower bound of s_0 by evaluating f at different points using an exponential grid (e.g. evaluating f in $s = 1, -1, 2, -2, 2^2, -2^2, 2^4, -2^4, \dots$). Once such bounds are found, one can perform a dichotomic search inside these bounds to find the root s_0 of f . This dichotomic search has a linear convergence of order 2, with each step summarized in Algorithm 2. It is important to note that this algorithm is correct even if f is not increasing, as long as $f(s) < 0$ when $s < s_0$ and $f(s) > 0$ when $s > s_0$, as is the case in this work when f is the derivative of the negative YJ log-likelihood.

Figure 6 is an illustration of EXPYJ that is based on exponential search.

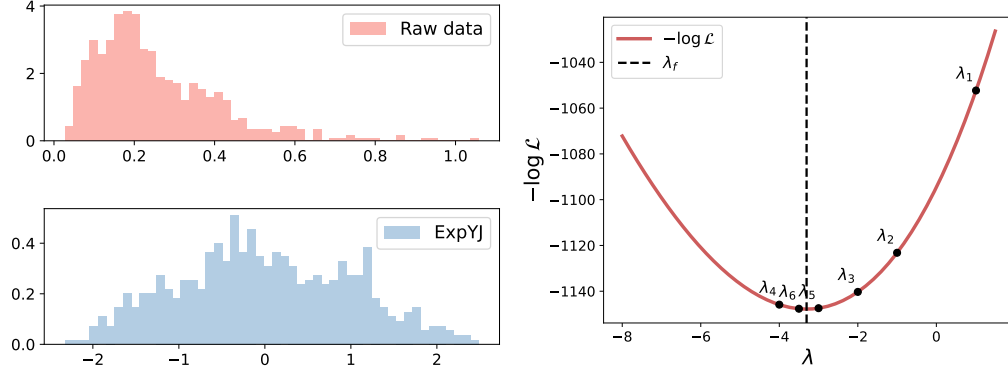


Figure 6: An example of EXPYJ applied to the largest perimeter of the cells in each sample of the *Breast Cancer* dataset. *Left*: histogram of the pooled dataset before (*top*) and after (*bottom*) applying a YJ transformation with fitted parameters. *Right*: negative log-likelihood of the YJ transformation as a function of λ . The points λ_t correspond to the values taken by EXPYJ during exponential search.

A natural extension of the exponential search is to replace the binary search into a k -ary search during the dichotomic search. In that case, $k - 1$ values of f are computed at each round. Such a modification reduces the number of steps required for a given accuracy while increasing the number of operations performed at each step.

C Proof of Proposition 3.1

We first introduce some lemmas that will be required for the main proof.

Lemma C.1. *Let $\lambda \mapsto f_i(\lambda)$, $i = 1, \dots, I$ be positive and twice differentiable functions, such that for all i , $\lambda \mapsto \ln[f_i(\lambda)]$ is convex. Then $\lambda \mapsto \ln[\sum_{i=1}^I f_i(\lambda)]$ is also convex.*

Proof. The proof of Lemma C.1 is based on the following lemma:

Lemma C.2. *Let $\{a_i\}_{i=1 \dots I}, \{b_i\}_{i=1 \dots I}, \{c_i\}_{i=1 \dots I}$ be real numbers, such that for all $1 \leq i \leq I$: $a_i \geq 0$, $b_i \geq 0$ and $a_i b_i \geq c_i^2$. Then*

$$\left(\sum_{i=1}^I a_i \right) \left(\sum_{i=1}^I b_i \right) \geq \left(\sum_{i=1}^I c_i \right)^2.$$

Indeed, it holds,

$$\left(\sum_{i=1}^I a_i \right) \left(\sum_{i=1}^I b_i \right) - \left(\sum_{i=1}^I c_i \right)^2 = \left(\sum_{i=1}^I a_i b_i - c_i^2 \right) + \left(\sum_{i=1}^I \sum_{i < j \leq I} a_i b_j + a_j b_i - 2c_i c_j \right).$$

The first sum contains only non-negative terms as $\forall i, a_i b_i \geq c_i^2$. Recalling that $a_i \geq 0$ and $b_i \geq 0$, the second sum also contains non-negative terms as $a_i b_j + a_j b_i - 2c_i c_j \geq a_i b_j + a_j b_i - 2\sqrt{a_i b_i} \sqrt{a_j b_j} = (\sqrt{a_i b_j} - \sqrt{a_j b_i})^2 \geq 0$

Now let us prove Lemma C.1. The convexity and twice differentiability of $\ln[f_i(\lambda)]$ implies that $\partial_\lambda^2 \ln[f_i(\lambda)] \geq 0$ and therefore that

$$f_i \partial_\lambda^2 f_i - (\partial_\lambda f_i)^2 \geq 0. \quad (6)$$

As $f_i > 0$, we can conclude from Eq. 6 that $\partial_\lambda^2 f_i \geq 0$. Using Lemma C.2 and the linearity of the derivative, we have:

$$\left(\sum_i f_i \right) \partial_\lambda^2 \left(\sum_i f_i \right) - \left(\partial_\lambda \sum_i f_i \right)^2 \geq 0.$$

which means that $\partial_\lambda^2 \ln(\sum_i f_i) \geq 0$. □

Lemma C.3. *Let $\{\alpha_i\}_{i=1, \dots, n_\alpha}$ and $\{\beta_i\}_{i=1, \dots, n_\beta}$ be two non-empty sets of real numbers, and let us denote $\{\gamma_i\}_i = \{\alpha_1, \dots, \alpha_{n_\alpha}, \beta_1, \dots, \beta_{n_\beta}\}$ and $n_\gamma = n_\alpha + n_\beta$. Let $\bar{\alpha} = \frac{1}{n_\alpha} \sum_i \alpha_i$, $\bar{\beta} = \frac{1}{n_\beta} \sum_i \beta_i$, $\bar{\gamma} = \frac{1}{n_\gamma} \sum_i \gamma_i$ and $\sigma_\alpha^2 = \frac{1}{n_\alpha} \sum_i (\alpha_i - \bar{\alpha})^2$, $\sigma_\beta^2 = \frac{1}{n_\beta} \sum_i (\beta_i - \bar{\beta})^2$, $\sigma_\gamma^2 = \frac{1}{n_\gamma} \sum_i (\gamma_i - \bar{\gamma})^2$. Then:*

$$\sigma_\gamma^2 = \frac{n_\alpha}{n_\gamma} \sigma_\alpha^2 + \frac{n_\beta}{n_\gamma} \sigma_\beta^2 + \frac{n_\alpha n_\beta}{n_\gamma^2} (\bar{\alpha} - \bar{\beta})^2.$$

Proof. This identity is easily obtained using the definitions of σ_α^2 , σ_β^2 and σ_γ^2 . □

C.1 Proof of Proposition 3.1

Proof. We start by proving the only shows the convexity of $-\log \mathcal{L}_{\text{YJ}}(\lambda)$, and prove strict convexity in Appendix C.4.

Let $\{x_i\}_{i=1 \dots n}$ be our data points and let us split this dataset into non-negative values $\{x_i^+\} = \{x_i | x_i \geq 0\}$ and negative values $\{x_i^-\} = \{x_i | x_i < 0\}$. Let $\gamma_i = \Psi(\lambda, x_i)$, $\alpha_i = \Psi(\lambda, x_i^+)$, and $\beta_i = \Psi(\lambda, x_i^-)$. We denote $n_\alpha, n_\beta, n_\gamma$ the lengths of the sets $\{\alpha_i\}$, $\{\beta_i\}$ and $\{\gamma_i\}$. For clarity, let us consider the case where both $\{x_i^+\}$ and $\{x_i^-\}$ have at least two distinct items and therefore $n_\alpha \geq 1$, $n_\beta \geq 1$ and $\sigma_\alpha^2 > 0$, $\sigma_\beta^2 > 0$. We relegate to Appendix C.3 the other edge cases. According to Lemma C.3, the expression of negative log-likelihood of the YJ transformation provided in Eq. (2) can be reformulated as:

$$\begin{aligned} -\log \mathcal{L}_{\text{YJ}}(\lambda) &= \frac{n}{2} \log(2\pi) - (\lambda - 1) \sum_{i=1}^n \text{sign}(x_i) \log(|x_i| + 1) \\ &\quad + \ln \left(\frac{n_\alpha}{n_\gamma} \sigma_\alpha^2 + \frac{n_\beta}{n_\gamma} \sigma_\beta^2 + \frac{n_\alpha n_\beta}{n_\gamma^2} (\bar{\alpha} - \bar{\beta})^2 \right). \end{aligned} \quad (7)$$

The first term is constant and the second one is linear in λ so we only have to prove the convexity of the last term to prove that the full negative log-likelihood is convex. Using Lemma C.1, we only need to show that $\lambda \mapsto \ln \left(\frac{n_\alpha}{n_\gamma} \sigma_\alpha^2 \right)$, $\lambda \mapsto \ln \left(\frac{n_\beta}{n_\gamma} \sigma_\beta^2 \right)$ and $\lambda \mapsto \ln \left(\frac{n_\alpha n_\beta}{n_\gamma^2} (\bar{\alpha} - \bar{\beta})^2 \right)$ are convex. We can get rid of the constant factor and show that $\lambda \mapsto \ln(\sigma_\alpha^2)$, $\lambda \mapsto \ln(\sigma_\beta^2)$ and $\lambda \mapsto \ln((\bar{\alpha} - \bar{\beta})^2)$ are convex.

The key idea of the proof is to use the fact that, according to [26], for any set of positive real numbers $\{a_i\}$, $\lambda \mapsto \ln \sigma[\Phi(\lambda, \{a_i\})]$ is convex, where $\Phi(\lambda, \cdot)$ denotes the Box-Cox transformation. Besides we have (see Appendix A.2):

$$\alpha_i = \Psi(\lambda, x_i^+) = \Phi(\lambda, x_i^+ + 1), \quad (8)$$

$$\beta_i = \Psi(\lambda, x_i^-) = -\Phi(2 - \lambda, 1 - x_i^-). \quad (9)$$

Therefore $\ln \sigma[\alpha_i] = \ln \sigma[\Phi(\lambda, (x_i^+ + 1))]$ which is a convex function of λ . Similarly, $\sigma[\{-\Phi(2 - \lambda, 1 - x_i^-)\}]^2 = \sigma[\{\Phi(2 - \lambda, 1 - x_i^-)\}]^2$. The function $\lambda \mapsto \sigma[\{\Phi(2 - \lambda, 1 - x_i^-)\}]^2$ is convex as the composition of the linear function $\lambda \mapsto 2 - \lambda$ with the convex function $\lambda \mapsto \sigma[\{\Phi(\lambda, 1 - x_i^-)\}]^2$.

Let us finally prove the convexity of $\lambda \mapsto \ln [(\bar{\alpha} - \bar{\beta})^2]$. We recall that $\bar{\alpha} > 0$ and $\bar{\beta} < 0$ and that $\ln [(\bar{\alpha} - \bar{\beta})^2] = 2 \ln [\bar{\alpha} - \bar{\beta}]$. Using Lemma C.1, we only need to prove that $\lambda \mapsto \ln (\bar{\alpha})$ and $\lambda \mapsto \ln (-\bar{\beta})$ are convex. As $\bar{\alpha}$ and $\bar{\beta}$ are defined as sums, still using Lemma C.1, we only need to prove that $\lambda \mapsto \ln (\Psi(\lambda, x_i^+))$ and $\lambda \mapsto \ln (-\Psi(\lambda, x_i^-))$ are convex for any i . Using, Eqs. (8) and (9), it is sufficient to prove that for any real number $a \geq 1$, the function $\lambda \mapsto \ln[\Phi(\lambda, (a))] = \ln[(a^\lambda - 1)/\lambda]$ is convex, which is proved in Appendix C.2. \square

C.2 Proof that $\lambda \mapsto \ln[\Phi(\lambda, (a))]$ is convex

Let $a \geq 1$ $u(\lambda) = (a^\lambda - 1)/\lambda$ and $g(\lambda) = \ln u(\lambda)$. For $\lambda \neq 0$, the second derivative of g is positive if and only if $D \stackrel{\text{def}}{=} \lambda^4(uu'' - (u')^2) \geq 0$.

We have

$$D(a, \lambda) = a^{2\lambda} - a^\lambda \lambda^2 \log(a)^2 - 2a^\lambda + 1.$$

Let us show that $D \geq 0$ when $\lambda \neq 0$. $D(a = 1, \lambda) = 0$, so we just need to show that $\partial_a D(a, \lambda) > 0$ when $a > 0$. As

$$\partial_a D(a, \lambda) = a^{(\lambda-1)} \lambda (2a^\lambda - \lambda^2 \log(a)^2 - 2\lambda \log(a) - 2),$$

let us define $T(a, \lambda)$ as:

$$T(a, \lambda) = (2a^\lambda - \lambda^2 \log(a)^2 - 2\lambda \log(a) - 2).$$

We just need to show that $T(a, \lambda) > 0$ when $\lambda > 0$ and $T(a, \lambda) < 0$ when $\lambda < 0$. As $T(a, 0) = 0$, we just need to show that $\partial_\lambda T(a, \lambda) > 0$ when $\lambda \neq 0$.

$$\partial_\lambda T(a, \lambda) = 2(a^\lambda - \lambda \log(a) - 1) \log(a).$$

As $a > 1$, $\log(a) > 0$, so we just need to show that $(a^\lambda - \lambda \log(a) - 1) > 0$ which can be done by replacing x by $\lambda \log(a)$ in the following inequality: $\exp(x) > x + 1$ for $x > 0$.

To conclude, when $\lambda \neq 0$ and $a \geq 1$, $D(\lambda, a) \geq 0$, and if $a > 1$ then $D(\lambda, a) > 0$. Therefore, the second derivative of g is positive for any $\lambda \geq 0$. Using continuity, we can conclude that the second derivative of g is positive for any λ and that $\lambda \mapsto \ln[\Phi(\lambda, (a))]$ is convex.

Note that if $a > 1$, then $D > 0$ and we can conclude that $\lambda \mapsto \ln[\Phi(\lambda, (a))]$ is strictly convex.

C.3 Edge cases not covered by the main proof of Proposition 3.1

In the main proof we assume that $n_\alpha \geq 2$, $n_\beta \geq 2$ and that $\sigma_\alpha^2 > 0$, $\sigma_\beta^2 > 0$. Said otherwise, we assume that both $\{x_i^+\}$ and $\{x_i^-\}$ have at least two distinct elements. The proof is almost unchanged if this is not the case, as we can discard any term inside the logarithm of Eq. 7. For example, let's assume that $n_\alpha = 1$. Therefore $\sigma_\alpha^2 = 0$. We can then rewrite Eq. 7 as:

$$\begin{aligned} -\log \mathcal{L}_{\text{YJ}} &= \frac{n}{2} \log(2\pi) - (\lambda - 1) \sum_{i=1}^n \text{sign}(x_i) \log(|x_i| + 1) \\ &\quad + \ln \left(\frac{n_\beta}{n_\gamma} \sigma_\beta^2 + \frac{n_\alpha n_\beta}{n_\gamma^2} (\bar{\alpha} - \bar{\beta})^2 \right). \end{aligned}$$

We only need to show that $\lambda \mapsto \ln \left(\frac{n_\beta}{n_\gamma} \sigma_\beta^2 \right)$ and $\lambda \mapsto \ln \left(\frac{n_\alpha n_\beta}{n_\gamma^2} (\bar{\alpha} - \bar{\beta})^2 \right)$ are convex as in the main proof.

Any other edge case can be treated similarly, and the proof holds as soon as $\{x_i\}$ has at least two distinct elements.

C.4 Strict convexity of the Yeo-Johnson negative log-likelihood.

To prove the strict convexity of the YJ negative log-likelihood, let us notice that under the hypotheses of Lemma C.1, if at least one function $\lambda \mapsto \ln(f_i)$ is strictly convex, then $\lambda \mapsto \ln[\sum_i f_i(\lambda)]$ is

strictly convex. Besides, according to [26], for any set of positive real $\{a_i\}$ with at least two distinct elements, $\lambda \mapsto \ln \sigma[\Phi(\lambda, (a_i))]$ is strictly convex. Therefore, in the case where either $\{x_i^+\}$ or $\{x_i^-\}$ has two distinct elements, we can conclude that the YJ negative log-likelihood is strictly convex.

The only problematic case is when both $\sigma_\alpha^2 = 0$ and $\sigma_\beta^2 = 0$. In that case $\{x_i\}$ has only two distinct element: one positive or null and one strictly negative. In that case, $\lambda \mapsto \sigma[\{\Phi(\lambda, 1 - x_i^-)\}]^2$ is strictly convex as $\lambda \mapsto \ln[\Phi(\lambda, (a)) = \ln[(a^\lambda - 1)/\lambda]$ is strictly convex for $a > 1$.

D Secure Multi-Party Computation

D.1 Shamir Secret Sharing

Secure Multiparty Computation (SMC) consists in evaluating functions without disclosing their inputs. One way to achieve this result is to use secret sharing. The main idea is that a value h is split into different secret shares $h_k, k = 1, \dots, K$ where K is the number of clients. Each client k only knows the value of the secret share h_k , and one needs at least p shares with $1 < p \leq K$ to recover the initial value h . The set of the secret shares h_k of h is denoted $\llbracket h \rrbracket$. Schematically, SMC consists in three main steps: (i) *secret sharing*, where each client splits its input into secret shares and sends them to the other clients (ii) *computation*, where the clients perform mathematical computations on the secret shares and obtain secret shares of the output and (iii) *reveal* steps, where the clients send each other the secret shares of the output in order to reconstruct and reveal the output.

In the Shamir Secret Sharing method [44], the secret shares of h correspond to the values of a given polynomial $P_h(x)$ of order K at different points x_k where $P_h(0) = h$. The values x_k are arbitrarily chosen by the protocol with the constraint that all x_k should be distinct. If all the clients disclose their secret share $h_k = P_h(x_k)$, then the secret h can be recovered by polynomial interpolation. In this framework the addition can be done trivially. If $\llbracket h \rrbracket = \{h_k\}_{k=1, \dots, K}$ and $\llbracket g \rrbracket = \{g_k\}_{k=1, \dots, K}$ are the shares of g , then $\llbracket g + h \rrbracket = \{g_k + h_k\}_{k=1, \dots, K}$ are shares of $g + h$. Said otherwise, $\llbracket g + h \rrbracket = \llbracket g \rrbracket + \llbracket h \rrbracket$. Therefore adding two shared secrets requires no communication between the clients. Similarly, multiplying a shared secret by a public constant c is done without communication as $\llbracket cg \rrbracket = c\llbracket g \rrbracket$. However, multiplying two shared secrets, i.e. computing shares of $\llbracket gh \rrbracket$ is more involved and requires one round of communication. More precisely, each client has to send one scalar quantity to all the other clients during this process, as explained for example in [37], section 3.

D.2 Fixed-Point Representation

The secret shares in SMC belong to a finite set \mathbb{Z}_p where p is a prime number and all the operations are integer operations done modulo p . In practice we consider integers encoded using l bits, then we choose the smallest prime number p such that $2^l < p$ and we perform each operation modulo p . Therefore any value has to be encoded as an integer using a finite number of bits. To encode negative integers, we consider that encoded integers between 0 and $2^{l-1} - 1$ are positive and encoded integers between 2^{l-1} and $2^l - 1$ are negative. We have to choose a value of l large enough such that the highest absolute value considered is below 2^{l-1} . Real-value numbers are encoded using fixed-point precision, as described in [8], where the f least significant bits of the encoding correspond to the decimal part, and the $l - f$ most significant bits correspond to the integer part. The addition of two fixed-point numbers in SMC can be done as described in Appendix D.1. However, multiplying two fixed-point representation numbers in SMC is more complex as the result must be divided by 2^f , i.e. the 2^f least significant bits are discarded. As explained in detail in [8], multiplying two fixed-point numbers requires two rounds of communication (instead of one round of communication for the multiplication of two integers).

D.3 Comparison in SMC

In SECUREFEDYJ, we need to compute in SMC the sign of an expression, which is equivalent to making a comparison with 0. As we are using fixed-point representation encoding, computing the sign amounts to computing the most significant bit of the binary decomposition of a given shared secret. In order to do so, we use the method described in [38], which works for any SMC framework supporting addition and multiplication. This method requires 10 rounds of communication among the clients (6 of which can be done offline, i.e. they correspond to random values exchanged

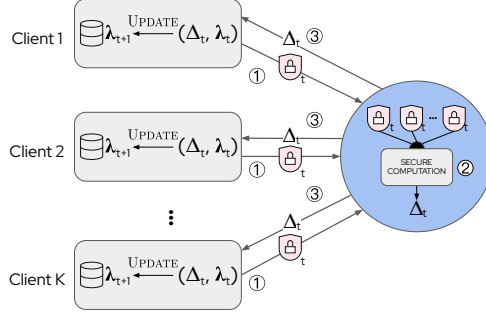


Figure 7: Simplified view of one round of SECUREFEDYJ. ①: All clients compute local, data-dependent quantities. ②: Δ_t is computed using SMC. Data-dependent quantities computed by each client are not disclosed during the process. ③: Δ_t is disclosed to all the clients, a new value λ_{t+1} is computed using an exponential update.

beforehand and can be done regardless of the value of the input). During these 10 rounds of communication, $153l + 423 \log l + 24$ multiplications are performed, $135l + 423 \log l + 16$ of which can also be done offline. Notice that other SMC primitives could be used, such as the one described in [17] which provides more efficient way to do SMC comparison.

D.4 MPyC

To implement SECUREFEDYJ we used the python library MPyC [42]. MPyC is based built upon VIFF framework [11] and is based on Shamir Secret Sharing [44]. We refer to [30] for a discussion of the performance of this library for various SMC tasks.

D.5 Further details on Algorithm 3

The pseudo-code provided in Algorithm 3, is a schematic overview of SECUREFEDYJ and relies on the SMC routines described above. For example, the following line of the pseudo-code:

$$\llbracket S_\varphi \rrbracket = \sum_k \llbracket S_{k,\varphi} \rrbracket$$

implies that: (i) each client k computes $S_{k,\varphi}$, divide it into secrets and send these share secrets to all the other clients; (ii) Using the SMC routines described in Appendices D.1, D.2 and D.4, the clients compute together the share secrets of $\llbracket S_\varphi \rrbracket$ where $S_\varphi = \sum_k S_{k,\varphi}$. After this step in Algorithm 3, the value of S_φ is therefore shared using share secrets across all the clients. Notice that the server only plays an orchestration roles in this process.

D.6 Complexity of SECUREFEDYJ

At each step of the exponential search, we share 6 secrets (the values of S_g), perform 10 fixed-point multiplications (including multiplying and dividing by n), and one comparison (i.e. computing the sign of $\partial_\lambda \mathcal{L}_{YJ}$).

The 6 secrets can be shared in parallel in one round of communication. Some of the multiplications can also be done in parallel, and only 3 successive rounds of multiplications have to be performed, which require 6 rounds of communications. As stated in Appendix D.3, the comparison requires 10 rounds of communications. Revealing the secret Δ also requires one round of communication. Notice that the additions do not require any round of communication. This amounts to 18 communications per exponential search step. Besides, computing $\llbracket S_\phi \rrbracket$ at the beginning of the algorithm and computing and revealing μ_* and σ_*^2 at the end of the algorithm requires 6 more rounds of communication. Overall, performing 40 steps of exponential search with SECUREFEDYJ costs $18 \times 40 + 6 = 726$ rounds of communications.

For each elementary operation, such as sharing a secret, revealing a secret or making a multiplication, the order of magnitude of the size of the message sent by each client to the other clients is $\lceil \log_2(p) \rceil$

bits. Notice that $\log_2(p)$ is of the same order of magnitude of l as p is the smallest prime number above 2^l . More precisely, each client sends around l bits to each of the other clients for these elementary operations. The overall size of the messages exchanged during the 726 rounds of communications mentioned above is mainly dominated by the $153l + 423 \log l + 24$ multiplications done at each of the 40 comparisons. Taking $l = 100$, we find that each client sends overall around $6.5 \cdot 10^7$ bits (or ~ 8 Mega-bytes) to each of the other clients during SECUREFEDYJ.

E Details of the numerical experiments

E.1 Datasets used in this work

Datasets exposed by *scikit-learn* API used in Figure 2 and Figure 3 For numerical experiments, we use four public datasets available in the UC Irvine Machine Learning repository [15] under a Creative Commons Attribution 4.0 International (CC BY 4.0) license and exposed by the *scikit-learn* datasets API. These datasets are the *Iris dataset* [18] (150 samples, 4 features), the *Wine Data Set* (178 samples, 13 features), the *Optical Recognition of Handwritten Digits Data Set* (1797 samples, 64 features) and the *Breast Cancer Wisconsin (Diagnostic) Data Set* (569 samples, 30 features). Only keeping features that have at least two distinct values, these datasets provide a total of 108 different features.

Extra UC Irvine Machine Learning repositories used to test Brent minimization method

Genomic data used in Figure 4 For genetic experiments, we rely on RNA-seq expression data from The Cancer Genome Atlas, expressed in Fragments per Kilobase Million (FPKM). We focus on 3 cancers: colorectal cancer (COAD), lung cancer (LUAD + LUSC), and pancreatic adenocarcinoma (PAAD). These datasets are available on <https://portal.gdc.cancer.gov/> under Open Access.

E.2 Experiments on TCGA data

Based on FPKM counts, we load all available data for each cancer of interest, removing genes with null expression for all samples.

Pipeline Our pipeline consists of three steps:

1. Normalization: either *whitening*, *log*, or Yeo-Johnson transformation;
2. Dimensionality reduction: a PCA was applied on normalized data to reduce dimension (dimension 128 for lung and colorectal cancer, 90 for pancreatic cancer);
3. Cox Proportional Hazards (CoxPH) [10] model fitting.

Normalization All normalization steps are performed on counts, regardless of the genes, as counts are related to the same underlying phenomenon induced by next-generation RNA sequencing. In other words, for the plain whitening, a single mean and variance is computed. For *log*, following application of $\log(1 + \cdot)$ to all entries, a similar count-level whitening is performed. For the YJ transformation, we perform 10 iterations of the proposed algorithm.

CoxPH model training CoxPH models are fitted with *lifelines* (0.26.4). We use an ℓ_2 regularization of magnitude 10 for each cancer, without any hyperparameter optimization.

Cross-validation Results are computed following 5-fold stratified group cross-validation, repeated 5 times with different seeds. Stratification is performed to ensure a balanced set of censored patients in each fold, while ensuring that samples belonging to the same patients end up in the same group to avoid over-estimating the generalization of the model.

E.3 Experiment on synthetic data

To generate the results of Section 5, we sampled for each of the 10 centers 200 datapoints using Eq. (4). We then apply an optional preprocessing steps before fitting a linear regression model using

Dataset name	# of samples	# of features (with at least two distinct values)	# of instabilities of Brent minimization
airfoil self noise	1503	5	0
blood transfusion	748	4	1
boston	506	13	0
breast cancer diagnostic	569	30	2
california	20640	8	0
climate model crashes	540	18	0
concrete compression	1030	7	0
concrete slump	103	7	0
connectionist bench sonar	208	60	0
connectionist bench vowel	990	10	0
ecoli	336	7	2
glass	214	9	0
ionosphere	351	34	0
iris	150	4	0
libras	360	90	0
parkinsons	195	23	0
planning relax	182	12	0
qsar biodegradation	1055	41	0
seeds	210	7	0
wine	178	13	0
wine quality red	1599	10	0
wine quality white	4898	11	0
yacht hydrodynamics	308	6	0
yeast	1484	8	0

Table 1: Number of feature for which the *scikit-learn* implementation of Yeo-Johnson based on Brent minimization method fails for 24 different datasets available on the UC Irvine Machine Learning repository [15]. We only kept the features with at least two distinct values.

scikit-learn *LinearRegression* model on the pooled data. Another dataset of 200 points was then generated, and we computed the R2 on this unseen dataset. This experiment was repeated 1000 times using each time a different seed and the box plot in Section 5 presents the min-max, the median the first and the third quartile. The different preprocessing steps shown are:

- None: no preprocessing step is applied
- Whitening: for each of the three dimensions of X_i , we subtract the empirical mean and we divide by the empirical standard deviation computed across all ten centers to the train dataset and the test dataset
- LocalYJ: we use one center randomly chosen to perform EXPYJ with $t_{\max} = 20$ to each of the dimensions of the dataset. The fitted triplets $\lambda_*, \mu_*, \sigma_*^2$ found for each column are then used to normalize the dataset of all 10 centers and the test dataset.
- Federated YJ: We apply SECUREFEDYJ with $t_{\max} = 20$ on the 10 centers to each of the dimensions of the dataset. The fitted triplets $\lambda_*, \mu_*, \sigma_*^2$ found for each column are then used to normalize the dataset of all 10 centers and the test dataset.

E.4 Testing Brent minimization on more dataset

As explained in the paragraph *Numerical stability of EXPYJ* of Section 3, applying blindly the Brent minimization method of *scikit-learn* to minimize the Yeo-Johnson negative log-likelihood might result in numerical instabilities and might collapse all the values of the dataset into a single value. To check further whether this phenomenon is likely to appear, we apply the *scikit-learn* Yeo-Johnson transformation to various real-life tabular datasets of the UC Irvine Machine Learning repository [15] (which are under a Creative Commons Attribution 4.0 International, CC BY 4.0). For each dataset, we only kept the features that have at least two distinct values. We found that for the 484 features out of 24 datasets, this issue arises 5 times, as summarized by Table 1

F Further details on Proposition 4.1

Proposition 4.1 states that all intermediate quantities of SECUREFEDYJ can be recovered from its final result λ_* . We provide in Algorithm 4 a way to construct the function \mathcal{F} introduced in Proposition 4.1 that can perform this recovery.

We apply Algorithm 4 on the 108 features used in Figure 3, with a fixed-point precision of $f = 50$. We numerically check that the output of \mathcal{F} from Algorithm 4 matches the intermediate quantities revealed by Algorithm 3 up to machine precision.

Algorithm 4 Function \mathcal{F} recovering quantities revealed by SECUREFEDYJ

Input: Hyperparameters $\lambda_{t=0}, \lambda_{t=0}^-, \lambda_{t=0}^+$ number of steps t_{\max}, λ_*

for $t = 1$ **to** t_{\max}

if $\lambda_{t-1} < \lambda_*$ **then**

$\Delta_t = 1$

else

$\Delta_t = -1$

end if

$\lambda_t, \lambda_t^-, \lambda_t^+ \leftarrow \text{EXPUPDATE}(\lambda_{t-1}, \lambda_{t-1}^-, \lambda_{t-1}^+, \Delta_t)$

end for

Output: $(\lambda_t, \lambda_t^-, \lambda_t^+, \Delta_t)_{t=0, \dots, t_{\max}}$
